International Journal of Environment and Geoinformatics 10(3):116-123 (2023)

Research Article

Google Earth Engine Based Spatio-Temporal Changes of Bafa Lake from 1984 to 2022

Omer Faruk Atiz*, Tansu Alkan, Suleyman Savas Durduran

Geomatics Engineering Department, Faculty of Engineering, Necmettin Erbakan University, Konya, Turkey

* Corresponding author: Ö.F.Atiz
E-mail: oatiz@erbakan.edu.tr

Received 27.02.2023
Accepted 09.09.2023

How to cite: Atiz et al., (2023). Google Earth Engine Based Spatio-Temporal Changes of Bafa Lake from 1984 to 2022, . *International Journal of Environment and Geoinformatics (IJEGEO)*, 10(3): 116-123. doi. 10.30897/ijegeo.1257413

Abstract

The water resource management is crucial to protect environment and ecological cycle. The detection of temporal and spatial changes in the lake's water extent is important for sustainable land planning. Therefore, the areal changes over the wetlands must be well monitored. Bafa Lake is an essential downstream water in the Büyük Menderes Basin which is the largest river basin of the Aegean Region. Google Earth Engine (GEE) is an easy-to-use cloud-based remote sensing data processing platform. In this study, the long-term spatio-temporal changes of Bafa Lake between 1984 and 2022 were analyzed using Landsat-5/8 satellite images on the GEE platform. A total of 1093 Landsat images were processed. The annual water areas were computed through composite images per year. The water areas extracted using the normalized water difference index (NDWI), modified NDWI (MNDWI), and automated water extraction index (AWEI). In the accuracy assessment according to random sampling points, the best results achieved with NDWI. For NDWI, Overall Accuracy (OA) was calculated as 98.03% and the kappa coefficient as 0.956. The minimum and maximum lake water areas in 38 years (NDWI) were detected as 5327 ha and 6725 ha in 1988 and 2019, respectively. In the past few years, the water area of Bafa Lake showed a stable variation.

Keywords: Google Earth Engine, Landsat, NDWI, Remote Sensing, Water Resources

Introduction

The ecosystem of our world has been drastically changed over the past years. The wetlands are the transition regions between terrestrial and aquatic ecosystems and are sometimes called the kidneys of the landscape (Mitsch and Gosselink, 2015). Therefore, the monitoring of the wetlands has unique importance. Environmental assets must be continuously monitored to make sustainable land management plans (Xu et. al., 2018). According to Ramsar's Global Wetland Outlook 2018 report, approximately one-third of wetlands have been lost since 1970 (Gardner and Finlayson, 2018). Numerous wetland areas (about three times the size of Van Lake) in Turkey have lost their ecological functions in the last 50 years (WWF, 2020).

The remote sensing method is successfully used for the extraction of water bodies. Landsat imageries are frequently used to create remote sensing time series due to the number of freely available datasets with broad temporal coverage (Banskota et. al., 2014). In the case of time series, the amount of data becomes large. This causes an increase in data processing time and computational burden. As a result, cloud-based remote sensing data processing platforms like Google Earth Engine (GEE) have become more popular (Gorelick et. al., 2017). The hardware limitations were eliminated, and much more remote sensing data could be processed.

The GEE platform is used in a broad range of monitoring applications, like urban expansion zones (Cao et. al., 2021; Khanal et. al., 2019; Kaya and Dervisoglu, 2023), climate change and air pollution (Ghasempour et. al., 2021; Bahsi et. al., 2022), land use and land cover (LULC) change (Loukika et. al., 2021; Pande, 2022), wetland areas (Kandekar et. al., 2021; Firatli et. al., 2022) and marine biosphere (Celik et. al., 2022; Li et. al., 2022; Çelik et al., 2022), forest fires and burned area mapping (Bar et. al., 2020; Arikan et. al., 2022; Yilmaz et. al., 2023), snow cover change (Notarnicola, 2020).

The spatial and temporal changes over a region can be found with different methods such as algebra-based, transform-based, classification-based, Geographical Information Systems (GIS), and advanced models (Asokan and Anitha, 2019). Image classification and spectral indices are widely used methods for detecting surface water (Firatli et al., 2022). The spectral water indices are efficient for detecting the water or non-water pixels (Albarqouni et. al., 2022).

There are several studies on the monitoring of global and regional wetland areas. Carrol et. al., 2009 produced a global water map at 250 m resolution. Verpoorter et. al., 2014 created a global lake inventory which consists of nearly 117 million lakes. Feng et. al., 2016 produced a global scale inland water body dataset with 30 m resolution. The main issue with the above global water body datasets is they generally cover relatively large wetlands. Moreover, some studies focused on the lakes in Turkey. Firatli et. al., 2022 investigated the natural lakes larger than 2000 ha in Turkey between 1985 and 2020 using GEE platform. They used the normalized difference

water index (NDWI) to extract lake water extents. Albarqouni et. al., 2022 assessed the Burdur, Egirdir, and Beysehir Lakes from the Lakes Region in Turkey between 2000 and 2021 years. They concluded that Burdur Lake is affected by human causes rather than climate conditions. Yagmur et. al., 2021 assessed the surface area changes of 18 natural lakes at Konya Closed Basin in Turkey between 1985 and 2015 years, using Landsat images. In Peker 2019, the spatio-temporal changes of the 16 lakes in the Lakes Region in Turkey were analyzed between 1984 and 2018 using Landsat and Sentinel 2 satellite images. The correlation with precipitation is found to be positive for the Lakes Eber, Ilgin, Beysehir, Acigol, Karatas, Akgol, Karamik and Gavur. Although several studies are conducted on a set of lakes, some studies investigate individual lakes and dams (Ormeci and Ekercin 2007; Temiz and Durduran 2016; Kale and Acarli 2019; Ates et. al., 2020; Topcu and Atatanir, 2021; Karaca et. al., 2022). Bafa Lake is an important lake in the Büyük Menderes Basin. Even though there are many studies on the monitoring of several lakes in Turkey, Bafa Lake has not been comprehensively investigated. In Topcu and Atatanir 2021, the temporal changes on the water surface area of the Bafa and Azap Lakes are examined. But they used different data sources as Landsat and Rapideye satellite images, orthophoto images, and topographical maps, covering the years 1987, 1999, 2007, 2014, and 2015. The usage of common datasets for different years provides homogeneity for the statistical analyses. The above study, use one image per year, instead of using a set of images. Further, the temporal coverage must be expanded.

This study aims to assess the spatio-temporal changes of Bafa Lake from 1984 to 2022 using Landsat-5/8 satellite images through the GEE cloud platform considering time series approach.

Study Area

In Turkey, there are 25 river basins (Figure 1a). Bafa Lake is a saline-brackish and an essential downstream water in the Büyük Menderes Basin which is the largest river basin of the Aegean Region. It is located between Aydin and Mugla province borders and at the south-east of the Büyük Menderes Basin (GDWM, 2017). The maximum depth of the lake is 21 m. The south and north sides of the lake are surrounded by mountains. The detailed location of the Bafa Lake is illustrated in Figure 1.

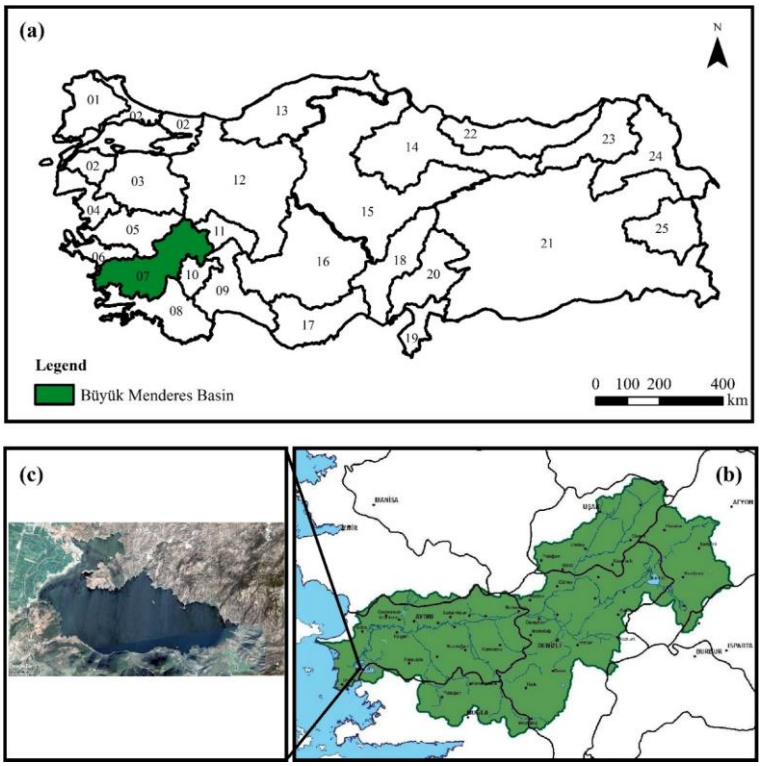

Fig. 1 The location of study area. a) River Basins in Turkey, b) Büyük Menderes Basin (Sahtiyanci, 2014), c) Google Earth Image.

In the lake area, there are several islands that have historical structures. Therefore, it has historical and cultural importance. Apart from them, the lake is registered as Nature Park and Class I Natural Protected area and has international importance. According to Tuna 2015, there are 180 possible bird species in the region, and hence the lake area has particular importance. Thus, the lake has the potential for ecotourism.

The domestic, industrial, and agricultural wastes collected through the Büyük Menderes River cause pollution in the lake. The water quality of Bafa Lake is classified as weak (Sahtiyanci, 2014). In 2006, there was a mass fish death in the lake due to human-induced effects (Erdogan 2011). As result, Bafa Lake must be well monitored to protect the ecosystem.

Data

Remote sensing involves taking images of the earth via remote sensors from artificial satellites, data analysis, and information extraction from these images. The spatio-temporal changes on Bafa Lake between 1984 and 2022 were evaluated using Landsat 5 TM (Thematic Mapper) and Landsat 8 OLI/ TIRS (Operational Land Imager/ Thermal Infrared Sensor) satellite images. These satellites have a temporal resolution of 16 days. Detailed information about the Landsat images is given in Table 1 (Landsat, 2023).

Table 1. Detailed information about Landsat-5/8 images

Satellite	Bands	Spectral Resolution (µm)	Spatial Resolution (m)
Landsat 5 TM (1984-2011)	B1 – Blue	0.45-0.52	30
	B2 – Green	0.52-0.60	30
	B3 – Red	0.63-0.69	30
	B4 – Near Infrared	0.76-0.90	30
	B5 – Shortwave Infrared-1	1.55-1.75	30
	B7 – Thermal Infrared	10.41-12.50	120
Landsat 8 OLI/ TIRS (2013-2022)	B1 – Coastal Aerosol	0.43-0.45	30
	B2 – Blue	0.45-0.51	30
	B3 – Green	0.53-0.59	30
	B4 – Red	0.64-0.67	30
	B5 – Near Infrared	0.85-0.88	30
	B6 – Shortwave Infrared-1	1.57-1.65	30
	B7 – Shortwave Infrared-2	2.11-2.29	30
	B8 – Panchromatic	0.50-0.68	15
	B9 – Cirrus	1.36-1.38	30
	B10 – Thermal Infrared-1	10.6-11.19	100
	B11 – Thermal Infrared-2	11.50-12.51	100
	B6 – Shortwave Infrared-2	2.08-2.35	30

Landsat 5 TM data was obtained from 1984 to 2011. Landsat 8 OLI satellite images are found from 2013 to 2023. For that reason, the 2012 year was discarded from the below analyses. In this study, the number of Landsat images used per year is shown in Figure 2. A total of 1093 satellite images were processed to extract water surface area changes.Apart from the Landsat imageries, the Google Earth high resolution image (Maxar) was used to evaluate the accuracy and efficiency of the study.

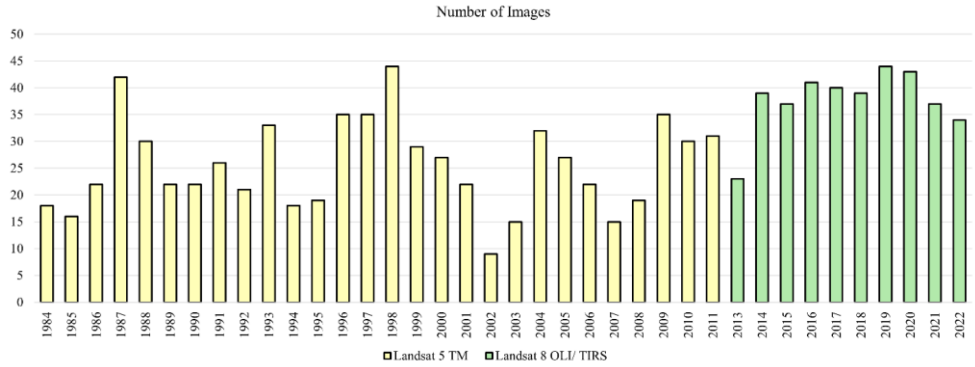

Fig. 2 The number of Landsat images

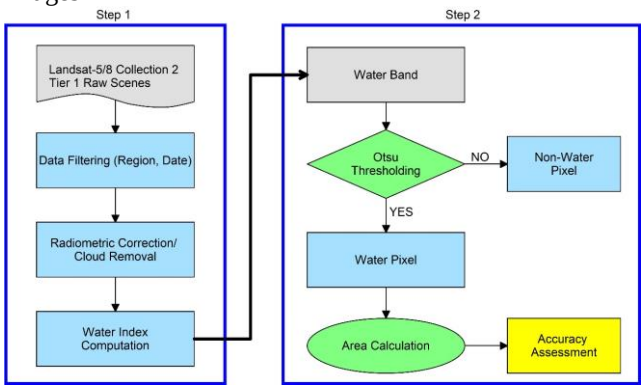

Fig. 3 The flowchart of the study

Method

The work was mainly conducted in three steps: data preparation, water area extraction, and accuracy assessment. The flowchart of the study is given in Figure 3. The Landsat Tier 1 Raw Images were used for their highest data quality. Tier 1 data is Level-1 Precision Terrain (L1TP) processed. Hence, they have well-characterized radiometry and are inter-calibrated across the different Landsat sensors (GEE, 2023a). After the data acquisition, a filter was applied according to the region of interest, cloud cover (less than 10%) and time. A Landsat algorithm in GEE (Landsat.simpleComposite) was used for radiometric correction and cloud removal (GEE, 2023b). This algorithm computes the cloud score for each pixel in the image collection and selects pixels with the least-cloud probability. So, the Landsat the top-of-atmosphere (TOA) composites per year computed from the image collection. After data pre-processing, the water extraction was conducted using NDWI, MNDWI, and AWEI.

NDWI was first presented in McFeeters 1996 to detect surface waters using green and NIR (Near Infrared)

bands. The surface waters are sensitive to the green band, in contrast to the NIR band. The formulation of NDWI is given below (McFeeters, 1996):

$$NDWI = \frac{BAND_{GREEN} - BAND_{NIR}}{BAND_{GREEN} + BAND_{NIR}} \quad (Eq.1)$$

According to Equation 1, the NDWI values are between -1 and +1 since the normalization. Xu 2006 developed a modified version of NDWI so-called MNDWI for better separation of built-up and water areas as formulated in Equation 2.

$$MNDWI = \frac{BAND_{GREEN} - BAND_{SWIR1}}{BAND_{GREEN} + BAND_{SWIR1}} \quad (Eq.2)$$

Apart from two band indices above Feyisa et. al., 2014, introduced a novel water extraction index named AWEI (Equation 3). AWEI has two forms, namely AWEI_sh and AWEI_nsh, and for areas with shadows, AWEI_sh is recommended (Feyisa et. al., 2014). In this study, AWEI_sh is used due to the mountains around the study area.

$$AWEI = BAND_{BLUE} + 2.5 * BAND_{GREEN} - 1.5 * (BAND_{NIR} + BAND_{SWIR1}) - 0.25 * BAND_{SWIR2} \quad (Eq.3)$$

The selection of a suitable threshold value is a major problem for index-based studies. In this study, dynamic thresholding with the Otsu method is applied. Otsu is a binarization method based on the selection of a value with maximum between-class variance (Otsu, 1979). Otsu thresholding improves the effectiveness of water extraction (Buma et. al., 2018). After the thresholding, water areas were computed over the classified NDWI, MNDWI, and AWEI water pixels. The accuracy assessment of classified images can be done with reference observations. In remote sensing, the reference data can be taken from higher resolution satellite images. Herein, an accuracy assessment was conducted over the water area of the 2019 year, using the high-resolution Maxar image as the reference. The Maxar image of the study area was taken from Google Earth software. The 303 random data points in the study area were manually compared to the high-resolution satellite image. The random data points are shown in Figure 4.

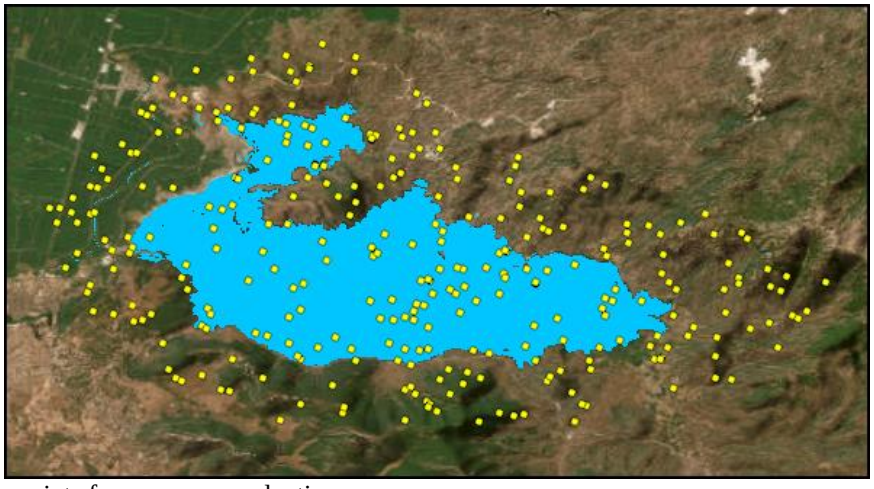

Fig. 4 The reference points for accuracy evaluation.

The binary confusion matrix was constructed as shown in Figure 5.

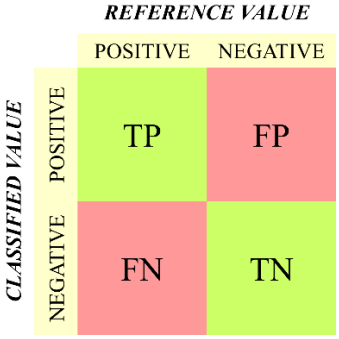

Fig. 5 The confusion matrix

In the confusion matrix TP, FP, FN, and TN values are defined as follows:
TP (True Positive): The correct classified water pixel.
TN (True Negative): The correct classified non-water pixel.
FP (False Positive): The misclassified water pixel.
FN (False Negative): The misclassified non-water water pixel.
The overall accuracy (OA), producer's accuracy (PA), user's accuracy (UA), and the Kappa coefficient (K) performance metrics may be calculated as given in the Equations 4-7 (Xia et. al., 2019; De Diego et. al., 2022).

$$OA = \frac{TP + TN}{TP + TN + FP + FN} \quad (Eq.4)$$

$$PA = \frac{TP}{TP + FN} \quad (Eq.5)$$

$$UA = \frac{TP}{TP + FP} \quad (Eq.6)$$

$$K = \frac{OA}{OA + \frac{(TP + TN) * (FP + FN)}{2 * (TP * TN - FP * FN)}} \quad (Eq.7)$$

The OA is a commonly used parameter for the general evaluation of classified pixels. Besides, the Kappa score provides information to check the classification model probability of agreement by chance (De Diego et. al., 2022).

Results and Discussion

Based on the above method, the annual water surface areas of Bafa Lake between 1984 and 2022 were calculated on the GEE. Then an accuracy evaluation was conducted to validate the method, using 2019 as a sample. The computed performance metrics are given in Table 2.

Table 2. The accuracy evaluation parameters (2019)

Parameter	NDWI	MNDWI	AWEI
Producer's accuracy (PA)	**98.08%**	95.19%	95.15%
User's accuracy (UA)	**96.23%**	96.12%	93.33%
Overall Accuracy (OA)	**98.03%**	97.04%	96.05%
Kappa coefficient (K)	**0.956**	0.934	0.912

According to Table 2., the method used in GEE provided remarkable accuracy for water area extraction. The best results were obtained with NDWI. The calculated annual water surface areas are provided in Figure 6. There are substantial variances in some years. This issue is mainly due to the shadows over the mountains around the study area. Visual interpretations were conducted to select the most suitable water index for the study area. Sample water index maps are provided in Figure 7. As seen in Figure 7, NDWI was selected as the most suitable index for Bafa Lake. Therefore, NDWI-based water areas were used at the below analysis and discussions. The mean water surface area of Bafa Lake between 1984-2022 was found as 6553 ha. However, the lake reached to 6725 ha in 2019, which is higher than the 2022 area by 1.74%. The minimum water area was found in 1988 as 5325 ha. This value is lower by 19.4% compared to 2022. The reason for the variations in the lake water area may be human-induced or environmental conditions. For further analyses of areal variations, the change percentages of each year according to the previous were calculated (Figure 8).

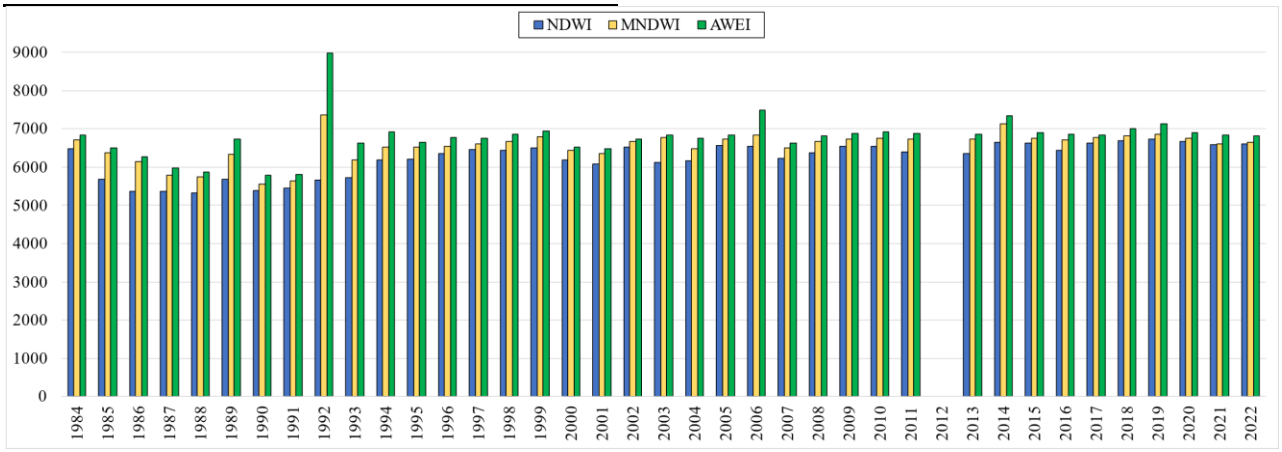

Fig. 6 Bafa Lake annual water surface areas

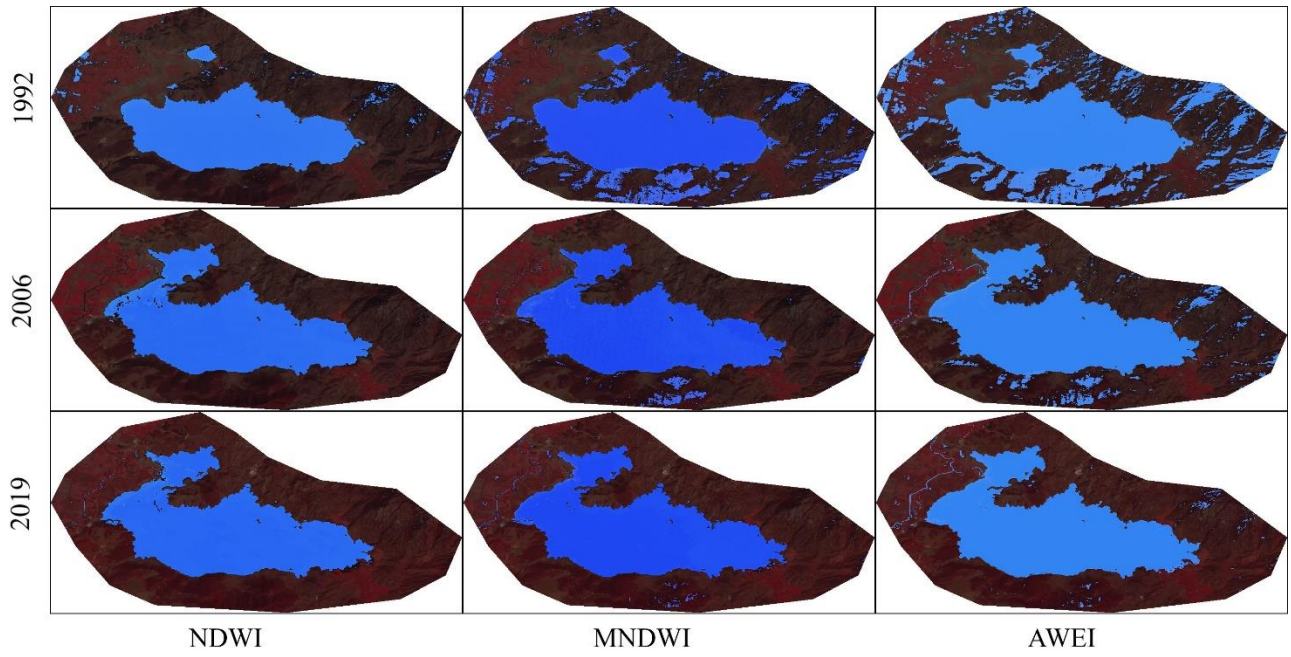

Fig. 7 Water surface areas at the sample years

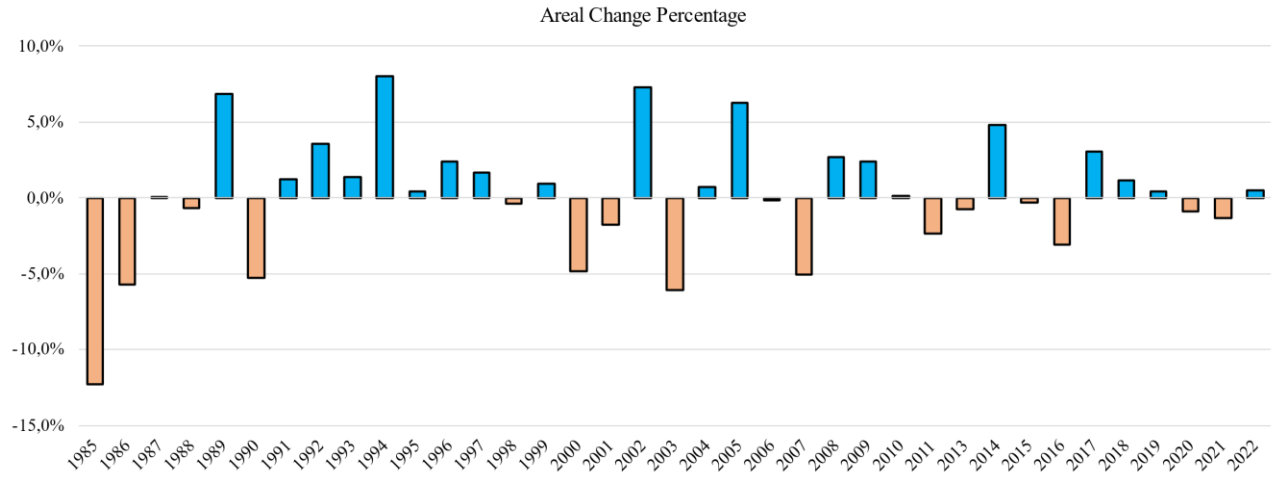

Fig. 8 NDWI areal change percentages (from previous year)

In Figure 8, the annual variations are better distinguishable. The highest decrease happened as much than 12%, in 1985. In 1985, a dam was built in the northern part of the lake to protect the settlements from potential flood hazards (Kucuksumbul, 2018). Thus, the lake could not be fed enough from the Büyük Menderes River. Sahtiyanci 2014, mentions that the surface water decrease is explained by the dam built in 1985. The lake was declared a Nature Protected area in 1994 after public pressure because of the water level decrease (Kucuksumbul, 2018). The decrease in 2007 can be explained by the dam and incorrect irrigation, as in the archive news (Hürriyet, 2007). After the year 2007, the maximum decrease was about %3. General Directorate of State Hydraulic Works announced a rubber dam project for the Bafa Lake in 2007 (SHW, 2007). The rubber dam was planned to transfer excess water from the Büyük Menderes River. The local authorities expressed the rubber dam is successfully used to compensate water level of Bafa Lake, especially in dry seasons (DEHA, 2012).
The linear trend model was applied to better express the variations in the water surface area. In Figure 9, the annual trend of Bafa Lake is shown.

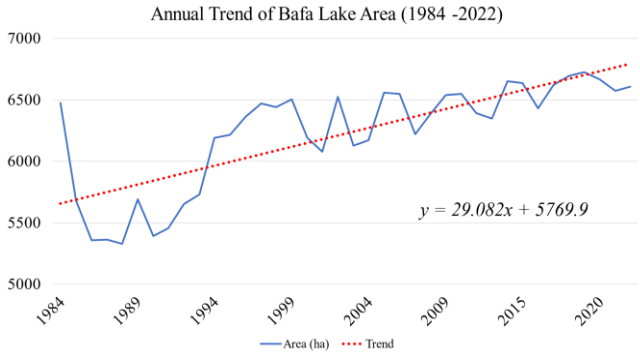

Fig. 9 Annual trend of water area change

It can be said that the annual trend can be unstable because of the feeding by the rubber dam.

Conclusions

In this study, the spatio-temporal changes of Bafa Lake during 1984-2022 were examined using Landsat 5 TM and Landsat 8 OLI satellite images based on GEE platform. The results showed that water areas of lakes can be well monitored with remarkable accuracy. It was found that Bafa Lake showed differences in surface area, and the reasons for that changes were discussed. The changes affected the ecology of the region. Besides, the variation in the water area was found to be slightly balanced in the past few years. The reduced variations demonstrated the effectiveness of the rubber dam. It can also be concluded that water resources management policies enhanced the water extent.
The method used in GEE can be easily adapted for other wetlands in different river basins. This can provide valuable information to decision-makers and may be helpful for other ecological policies. It can be noted that the continuous monitoring of several wetlands in Turkey is crucial to develop land management policies. However, the monitoring studies should be expanded by considering seasonal variations and climate conditions.

Acknowledgements

The authors would like to thank Google for providing the Google Earth Engine platform.

References

Albarqouni, M. M., Yagmur, N., Bektas Balcik, F., Sekertekin, A. (2022). Assessment of spatio-temporal changes in water surface extents and lake surface temperatures using Google Earth Engine for lakes region, Türkiye. *ISPRS International Journal of Geo-Information*, 11(7), 407.

Arikan, C., Tumer, I. N., Aksoy, S., Sertel, E. (2022). Determination of burned areas using Sentinel-2A imagery and machine learning classification algorithms. 4th Intercontinental Geoinformation Days (IGD), 43-46, Tabriz, Iran.

Asokan, A., Anitha, J. (2019). Change detection techniques for remote sensing applications: A survey. *Earth Science Informatics*, 12, 143-160.

Ates, A. M., Yilmaz, O. S., Gulgen, F. (2020). Using remote sensing to calculate floating photovoltaic technical potential of a dam's surface. *Sustainable Energy Technologies and Assessments*, 41, 100799.

Bahsi, K., Ustaoglu, B., Aksoy, S., Sertel, E. (2022). Estimation of emissions from crop residue burning in Türkiye using remotely sensed data and the Google Earth Engine platform. *Geocarto International*, 2157052.

Banskota, A., Kayastha, N., Falkowski, M. J., Wulder, M. A., Froese, R. E., White, J. C. (2014). Forest monitoring using Landsat time series data: A review. *Canadian Journal of Remote Sensing*, 40(5), 362-384.

Bar, S., Parida, B. R., Pandey, A. C. (2020). Landsat-8 and Sentinel-2 based forest fire burn area mapping using machine learning algorithms on GEE cloud platform over Uttarakhand, Western Himalaya. Remote Sensing Applications: *Society and Environment*, 18, 100324.

Buma, W. G., Lee, S. I., Seo, J. Y. (2018). Recent surface water extent of lake Chad from multispectral sensors and GRACE. *Sensors*, 18(7), 2082.

Cao, W., Zhou, Y., Li, R., Li, X., Zhang, H. (2021). Monitoring long-term annual urban expansion (1986–2017) in the largest archipelago of China. *Science of The Total Environment*, 776, 146015.

Carroll, M. L., Townshend, J. R., DiMiceli, C. M., Noojipady, P., Sohlberg, R. A. (2009). A new global raster water mask at 250 m resolution. *International Journal of Digital Earth*, 2(4), 291-308.

Çelik, O. I., Çelik, S. Gazioğlu, C. (2022). Evaluation on 2002-2021 CHL-A concentrations in the Sea of Marmara with GEE enhancement of satellite data. *International Journal of Environment and Geoinformatics*, 9(4), 68-77.

De Diego, I. M., Redondo, A. R., Fernández, R. R., Navarro, J., Moguerza, J. M. (2022). General performance score for classification problems. *Applied Intelligence*, 52(10), 12049-12063.

DEHA (2012). Deniz Haber Ajansı, Bafa Lake breathes with "Rubber Dam" (Bafa Gölü "Şişme Savak" ile nefes alıyor). Retrieved 24 February 2023 from https://www.denizhaber.net/

SHW (2007). General Directorate of State Hydraulic Works 2007 Activity Report (Devlet Su İşleri Genel Müdürlüğü 2007 Yılı Faaliyet Raporu).

Erdogan, S. (2011). A chemical reaction to a physical impact: Lake Bafa wetland ecosystem (Turkey) case. Ankara Üniversitesi Çevrebilimleri Dergisi, 3(1), 1-8.

Feng, M., Sfexton, J. O., Channan, S., Townshend, J. R. (2016). A global, high-resolution (30-m) inland water body dataset for 2000: First results of a topographic–spectral classification algorithm. *International Journal of Digital Earth*, 9(2), 113-133.

Feyisa, G. L., Meilby, H., Fensholt, R., Proud, S. R. (2014). Automated Water Extraction Index: A new technique for surface water mapping using Landsat imagery. *Remote Sensing of Environment*, 140, 23-35.

Firatli, E., Dervisoglu, A., Yagmur, N., Musaoglu, N., Tanik, A. (2022). Spatio-temporal assessment of natural lakes in Turkey. *Earth Science Informatics*, 15, 951-964.

Gardner, R.C., Finlayson, M. (2018). Global wetland outlook: State of the world's wetlands and their services to people 2018. Secretariat of the Ramsar Convention.

GDWM (2017). General Directorate of Water Management, Lakes and Wetlands Action Plan 2017-2023 (Su Yönetimi Genel Müdürlüğü, Göller ve Sulak Alanlar Eylem Planı 2017-2023).

GEE (2023a). Google Earth Engine Data Catalog.

GEE (2023b). Google Earth Engine API Reference.

Ghasempour, F., Sekertekin, A., Kutoglu, S. H. (2021). Google earth engine based spatio-temporal analysis of air pollutants before and during the first wave COVID-19 outbreak over Turkey via remote sensing. *Journal of Cleaner Production*, 319, 128599.

Gorelick, N., Hancher, M., Dixon, M., Ilyushchenko, S., Thau, D., Moore, R. (2017). Google Earth Engine: Planetary-scale geospatial analysis for everyone. *Remote Sensing of Environment*, 202, 18-27.

Hürriyet (2007). 1.3 million hectares of wetland lost (1.3 milyon hektarlık sulak alan kaybedildi). Retrieved 24 February 2023 from https://www.hurriyet.com.tr

Kale, S. Acarlı, D. (2019). Spatial and temporal change monitoring in water surface area of Atikhisar Reservoir (Çanakkale, Turkey) by using remote sensing and geographic information system techniques. *Alinteri Journal of Agriculture Science*, 34(1), 47-56.

Kandekar, V. U., Pande, C. B., Rajesh, J., Atre, A. A., Gorantiwar, S. D., Kadam, S. A., Gavit, B. (2021). Surface water dynamics analysis based on sentinel imagery and Google Earth Engine Platform: a case study of Jayakwadi dam. *Sustainable Water Resources Management*, 7(3), 44.

Karaca, M., Yagmur, N. Balcik, F. (2022). Determination of the temporal variation of Istanbul Terkos Lake using Google Earth Engine (İstanbul Terkos Gölü zamansal değişiminin Google Earth Engine kullanılarak belirlenmesi). *Geomatik*, 7(3), 235-242.

Kaya, Z., Dervisoglu, A. (2023). Determination of urban areas using Google Earth Engine and spectral indices; Esenyurt case study. *International Journal of Environment and Geoinformatics*, 10(1), 1-8.

Khanal, N., Uddin, K., Matin, M. A., Tenneson, K. (2019). Automatic detection of spatiotemporal urban expansion patterns by fusing OSM and Landsat data in Kathmandu. *Remote Sensing*, 11(19), 2296.

Kucuksumbul, A. (2018). Hydrogeological study of Söke Plain and Lake Bafa surroundings: Geothermal potential, soil and water contamination (Söke Ovası ve Bafa Gölü çevresinin hidrojeolojik incelenmesi: Jeotermal potansiyeli, toprak ve su kirliliği) (Master Thesis). Dokuz Eylül University the Graduate School of Natural and Applied Sciences, Izmir, Turkey.

LANDSAT (2023). NASA Landsat Technical Details.

Li, D., Gao, Z., Wang, Y. (2022). Research on the long-term relationship between green tide and chlorophyll-a concentration in the Yellow Sea based on Google Earth Engine. *Marine Pollution Bulletin*, 177, 113574.

Loukika, K. N., Keesara, V. R., Sridhar, V. (2021). Analysis of land use and land cover using machine learning algorithms on Google Earth Engine for Munneru River Basin, India. *Sustainability*, 13(24), 13758.

McFeeters, S. K. (1996). The use of the Normalized Difference Water Index (NDWI) in the delineation of

open water features. *International Journal of Remote Sensing*, 17(7), 1425-1432.

Mitsch, W. J., Gosselink, J. G. (2015). *Wetlands*. New Jersey: John Wiley & Sons.

Notarnicola, C. (2020). Hotspots of snow cover changes in global mountain regions over 2000–2018. *Remote Sensing of Environment*, 243, 111781.

Otsu, N. (1979). A threshold selection method from gray-level histograms. *IEEE Transactions on Systems, Man, and Cybernetics*, 9(1), 62-66.

Ormeci, C., Ekercin, S. (2007). An assessment of water reserve changes in Salt Lake, Turkey, through multi-temporal Landsat imagery and real-time ground surveys. *Hydrological Processes: An International Journal*, 21(11), 1424-1435.

Pande, C. B. (2022). Land use/land cover and change detection mapping in Rahuri watershed area (MS), India using the Google Earth Engine and machine learning approach. *Geocarto International*, 1-21.

Peker, E. A. (2019). Spatio-temporal changes of lake water extents in lakes region (Turkey) using remote sensing (Master's thesis), Middle East Technical University, Ankara, Turkey.

Sahtiyanci, O. H. (2014). Environmental targets and measures program under the water framework directive: The Case of the Büyük Menderes Basin (Su çerçeve direktifi kapsamında çevresel hedefler ve önlemler programı: Büyük Menderes Havzası örneği) (Specialist thesis). General Directorate of Water Management, Ankara, Turkey.

Temiz, F., Durduran, S. S. (2016). Monitoring coastline change using remote sensing and GIS technology: a case study of Acıgöl Lake, Turkey. In IOP Conference Series: Earth and Environmental Science (Vol. 44, No. 4, p. 042033). IOP Publishing.

Topcu, H. Atatanir, L. (2021). Determination of temporal variation in Bafa and Azap lake surface areas (Bafa ve Azap göl yüzey alanlarındaki zamansal değişimin belirlenmesi). *Akademik Ziraat Dergisi*, 10(1), 115-122.

Tuna, M. (2015). GEKA Project Report: Determination of community supported ecotourism activities in Lake Bafa Basin (Bafa Gölü havzasında toplum destekli ekoturizm faaliyetlerinin belirlenmesi).

Verpoorter, C., Kutser, T., Seekell, D. A., Tranvik, L. J. (2014). A global inventory of lakes based on high-resolution satellite imagery. *Geophysical Research Letters*, 41(18), 6396-6402.

WWF (2020). Annual Report 2020 Turkey (WWF Türkiye 2020 Faaliyet Raporu).

Xia, H., Zhao, J., Qin, Y., Yang, J., Cui, Y., Song, H., ... Meng, Q. (2019). Changes in water surface area during 1989–2017 in the Huai River Basin using Landsat data and Google Earth Engine. *Remote Sensing*, 11(15), 1824.

Xu, H. (2006). Modification of normalised difference water index (NDWI) to enhance open water features in remotely sensed imagery. *International Journal of Remote Sensing*, 27(14), 3025-3033.

Xu, X., Jiang, B., Tan, Y., Costanza, R., Yang, G. (2018). Lake-wetland ecosystem services modeling and valuation: Progress, gaps and future directions. *Ecosystem Services*, 33, 19-28.

Yagmur, N., Bilgilioglu, B. B., Dervisoglu, A., Musaoglu, N., Tanik, A. (2021). Long and short-term assessment of surface area changes in saline and freshwater lakes via remote sensing. *Water and Environment Journal*, 35(1), 107-122.

Yilmaz, O. S., Acar, U., Sanli, F. B., Gulgen, F., Ates, A. M. (2023). Mapping burn severity and monitoring CO content in Türkiye's 2021 Wildfires, using Sentinel-2 and Sentinel-5P satellite data on the GEE platform. *Earth Science Informatics*, 1-20.